

Identification of a New Class of PGT Inhibitors and Characterization of Their Biological  
Effects on PGE<sub>2</sub> Transport

Yuling Chi

Sonya M. Khersonsky

Young-Tae Chang

Victor L. Schuster

Albert Einstein College of Medicine, Departments of Medicine and of Physiology &  
Biophysics, 1300 Morris Park Ave, Bronx, NY (YC and VLS)

New York University, Department of Chemistry, 29 Washington Place, Room 551, New  
York, NY 10003 (SMK and Y-T Chang)

Running title: Inhibitors of prostaglandin transporter

Corresponding author:

Victor L. Schuster, M.D.  
Albert Einstein College of Medicine  
Belfer Bldg Room 1008  
1300 Morris Park Ave  
Bronx, NY 10461  
schuster@aecom.yu.edu  
telephone: 718-430-8560  
Fax: 718-430-8659

Text pages: 8

Tables: 1

Figures: 4 (plus 3 in Supplemental Data)

References: 41

Words in abstract: 131

Words in Introduction: 398

Words in Discussion: 591

Non-standard abbreviations:

COX, cyclooxygenase

GFP, green fluorescence protein

MCDK, Madin Darby Canine Kidney

MRP4, Multi Drug Resistance Protein 4

OAT, Organic Anion Transporter

PG, Prostaglandin

PGT, Prostaglandin transporter

## Abstract

Prostaglandins (PGs) are involved in several major signaling pathways. Their effects are terminated when they are transported across cell membranes and oxidized intracellularly. The transport step of PG metabolism is carried out by the prostaglandin transporter (PGT). Inhibition of PGT would therefore be expected to change local or circulating concentrations of prostaglandins, and thus their biological effects. To develop PGT-specific inhibitors with high-affinity, we designed a library of triazine compounds and screened 1,842 small molecules by using MDCK cells stably expressing rat PGT. We found several effective PGT inhibitors. Among them, the most potent inhibitor was TGBz T34, with a  $K_i$  of  $3.7 \pm 0.2 \mu\text{M}$ . These inhibitors allowed us to isolate the efflux process of  $\text{PGE}_2$  and to demonstrate that PGT does not transport  $\text{PGE}_2$  outwardly under physiological conditions.

## Introduction

Prostaglandins (PGs) are synthesized from arachidonic acid by cyclooxygenases (COX1 and COX2) and corresponding synthases (Helliwell et al., 2004). PGs play an important role in physiology and clinical settings. Their biological effects include triggering inflammation, fever and pain (Blatteis and Sehic, 1997; Bley et al., 1998; Vanegas and Schaible, 2001; Samad et al., 2002); induction of labor (Ulmann et al., 1992); modulation of renal hemodynamics and of water and solute reabsorption (Epstein, 1986; Wang et al., 1998; Yokoyama et al., 2002); and arterial vasodilatation (Clyman et al., 1978; Coceani and Olley, 1988; Smith et al., 1994). PG analogues, such as latanoprost and unoprostone, have been used to treat glaucoma (Stjernschantz, 1995; Alm, 1998; Susanna et al., 2002; Stjernschantz, 2004). At the cellular level, PGs are involved in several major signaling pathways, including the MAP kinase and protein kinase A pathways by upregulation of cAMP (Narumiya et al., 1999; Bos et al., 2004).

The magnitude of PG effects depends not only on their production but also their metabolism. We identified the prostaglandin transporter (PGT) (Kanai et al., 1995), and have reported that PGT removes PGs from the extracellular compartment and thereby terminates their interactions with receptors on cell membranes. PGT delivers PGs to cytoplasmic 15-OH PG dehydrogenase (Schuster, 2002; Nomura et al., 2004), resulting in oxidation and inactivation.

Because PGT is highly expressed in the tissues and organs where PGs are synthesized (Bao et al., 2002), and because PGT regulates a broad and complex PG signaling system, an inhibitor of PGT would be important for manipulating signaling. Known PGT blockers include inhibitors of the organic anion transporters (OATs), such

as bromocresol green and bromosulfophthalein, and some COX2 inhibitors, such as indomethacin and ibuprofen (Bito and Salvador, 1976; Kanai et al., 1995). One of the main problems with these inhibitors is that they are not specific for PGT (Jacquemin et al., 1994; Sweet et al., 1997). Thus a search for additional PGT inhibitors is indicated.

To develop high-affinity, PGT-specific inhibitors, we screened compounds from a triazine library. Using MDCK cells stably expressing PGT (Endo et al., 2002), screening of 1,842 small molecules yielded several effective inhibitors. The most potent inhibitor in this group of compounds, TGBz T34, has a  $K_i$  of  $3.7 \pm 0.2 \mu\text{M}$ . This compound also permitted us to isolate the efflux process of  $\text{PGE}_2$  transport and demonstrate that  $\text{PGE}_2$  influx and efflux are mediated by separate processes.

## Methods

### *Materials*

The cell lines used in this study were 3T3 cells that express endogenous PGT, and MDCK cells stably transfected with the GFP-tagged PGT in our laboratory (Endo et al., 2002). Tritium labeled PGE<sub>2</sub> ([<sup>3</sup>H]PGE<sub>2</sub>) was purchased from Perkin Elmer. Unlabeled PGE<sub>2</sub> was obtained from Cayman.

### *Synthesis of 1842 small molecule compounds*

The methods and procedures for synthesis of 1842 compounds were reported elsewhere (Moon et al., 2002; Bork et al., 2003a; Bork et al., 2003b; Khersonsky et al., 2003; Uttamchandani et al., 2004).

### *PGE<sub>2</sub> Transport Measurement*

MDCK or 3T3 cells were seeded at 15-20% confluence on 24-well plates. The day on which the cells were seeded was considered day 1. PGE<sub>2</sub> uptake experiments were conducted on day 4. All of the PGE<sub>2</sub> uptake experiments were conducted at room temperature. On day 4, cells were washed twice with Waymouth buffer (135 mM NaCl, 13 mM H-Hepes, 13 mM Na-Hepes, 2.5 mM CaCl<sub>2</sub>, 1.2 mM MgCl<sub>2</sub>, 0.8 mM MgSO<sub>4</sub>, 5 mM KCl, and 28 mM D-glucose). Then 200 μL of Waymouth buffer containing [<sup>3</sup>H]PGE<sub>2</sub> was added to each well. At the designed time, the uptake of [<sup>3</sup>H]PGE<sub>2</sub> was stopped by aspiration of uptake buffer; this was followed by immediate washing twice with 500 μL of chilled Waymouth buffer. Cells were then lysed with 100 μL lysis buffer containing 0.25% SDS and 0.05 N NaOH. 1.5 mL of scintillation solution was added to each well, and intracellular [<sup>3</sup>H]PGE<sub>2</sub> was counted by MicroBeta Counter.

For preliminary screening of the compounds, 25  $\mu\text{L}$  of Waymouth buffer containing small organic compounds were added to each well; this was immediately followed by the addition of 175  $\mu\text{L}$  of Waymouth buffer containing [ $^3\text{H}$ ]PGE<sub>2</sub>. In each well, the total volume of uptake medium was 200  $\mu\text{L}$ . Organic compounds were first dissolved in DMSO and then diluted in Waymouth buffer. The percent inhibition of [ $^3\text{H}$ ]PGE<sub>2</sub> uptake by compounds was calculated as  $[(\text{uptake}_{\text{vehicle}} - \text{uptake}_{\text{inhibitor}}) \div (\text{uptake}_{\text{vehicle}})] \times 100$ .

#### *Measurements of $K_i$ values*

The initial velocities at various initial extracellular concentrations of PGE<sub>2</sub> were determined from the PGE<sub>2</sub> uptake in the first 2 minutes; these were linear over the time course of PGE<sub>2</sub> uptake.  $K_i$  values were obtained by curve fitting the reciprocal of initial velocities of PGE<sub>2</sub> uptake versus the reciprocal of extracellular PGE<sub>2</sub> concentrations at various concentrations of the inhibitors. At low PGE<sub>2</sub> concentrations, the extracellular concentrations were taken as  $^3\text{H}$  labeled PGE<sub>2</sub>, which has a specific activity of 500  $\mu\text{Ci/mol}$ . At high concentrations of PGE<sub>2</sub>, we made a mixture of  $^3\text{H}$  labeled and unlabeled PGE<sub>2</sub> to a final specific activity of 25  $\mu\text{Ci/mol}$ .

## Results

### *Screening of small molecules for inhibition of PGE<sub>2</sub> uptake*

The small molecule triazine library compounds (1,842 members) were synthesized following reported procedures (Moon et al., 2002; Bork et al., 2003a; Bork et al., 2003b; Khersonsky et al., 2003; Uttamchandani et al., 2004). The main scaffolds of the compounds are depicted in Figure 1 with our codes of AA, BN, EA, RT, TF, and TGBz. The full structural information on R1 and R2 groups is provided in Supplemental Data, Figures 1S and 2S. Among the 1,842 compounds tested, the six compounds with the highest inhibitory activities were all from the TGBz scaffold. The T substituent at the R1 position and an acidic group (COOH or phenol) at the R2 position constitute important motifs for activity.

### *Determination of K<sub>i</sub> values of inhibitors and their modes of inhibition*

Of the six initial compounds, we chose TGBz T34, T07, and T41 (Figure 2) to further determine their inhibition kinetic parameters. Structures of the other three compounds are given in Supplemental Data, Figure 3S. The inhibition constant of TGBz T34 and its mode of inhibition, as determined by varying the PGE<sub>2</sub> concentrations at fixed levels of TGBz T34, are shown in Figure 3. The pattern was characteristic for competitive inhibition. The same experiments were conducted for TGBz T41 and T07; the K<sub>i</sub> values are listed in Table 1. All of these compounds are competitive inhibitors of PGT. TGBz T34 is the most potent inhibitor with a K<sub>i</sub> of 3.7 ± 0.2 μM. In separate experiments, when cells were pre-incubated in TGBz T34 for 10 or 20 minutes, the K<sub>i</sub> was not significantly different from that obtained by adding TGBz T34 simultaneously with PGE<sub>2</sub> (0 min pre-incubation K<sub>i</sub> = 1.22 μM; 10 min pre-incubation K<sub>i</sub> = 1.63 μM; 20



min pre-incubation  $K_i = 1.41 \mu\text{M}$ , NS to each other). These data suggest that there is no significant time dependency of binding of the inhibitor to PGT.

*TGBz T34 specifically inhibits PGE<sub>2</sub> uptake by PGT*

A typical time course of PGE<sub>2</sub> uptake in the absence of inhibitor is shown in Figure 4A (squares). In the absence of TGBz T34, intracellular PGE<sub>2</sub> rapidly accumulated, reaching a peak within 9 or 10 minutes. After this overshoot, a plateau was obtained, indicating that the rate of uptake equaled the rate of efflux. These data are similar to those previously published from our laboratory (Chan et al., 1998; Chan et al., 2002).

To further test the inhibition effect of TGBz T34, we measured the time course of PGE<sub>2</sub> uptake in the presence of various concentrations of TGBz T34 added at the beginning of uptake. As shown in Figure 4A, as the concentration of TGBz T34 increased, the peak level of intracellular PGE<sub>2</sub> accumulation decreased and the time point for reaching the peak PGE<sub>2</sub> level shifted, such that it took a shorter time for intracellular PGE<sub>2</sub> to reach its peak level at higher concentrations of TGBz T34. Also, as the concentration of TGBz T34 increased, the overshoot phenomenon diminished. When the concentration of TGBz T34 was 25  $\mu\text{M}$ , i.e. 8 fold higher than its  $K_i$ , the overshoot phenomenon completely disappeared. The residual uptake reflects PGE<sub>2</sub> entry by diffusion; it is similar to the curve of PGE<sub>2</sub> uptake by wild-type MDCK cells before they were transfected with PGT (Endo et al., 2002). Similar overshoot data and inhibition by TGBz T34 were obtained in Swiss 3T3 cells expressing endogenous PGT (data not shown).

*PGT does not export PGE<sub>2</sub>*

Since the discovery of PGT, the issue of whether it transports PGs in both directions has been unsettled (Chan et al., 1998; Schuster, 2002; Banu et al., 2003). To resolve this issue, we applied TGBz T34 after loading intracellular PGE<sub>2</sub> to a peak level (9 minutes) so as to block all PGE<sub>2</sub> transport by PGT, and then monitored the efflux of PGE<sub>2</sub>. As shown in Figure 4B, addition of TGBz T34 at 25 μM induced a rapid depletion of intracellular PGE<sub>2</sub>. Intracellular PGE<sub>2</sub> fell to baseline within 5 minutes and remained at that level for the rest of the time course. When there was no addition of T34, intracellular PGE<sub>2</sub> stayed at a much higher level. This result strongly suggests that PGT does not participate in PGE<sub>2</sub> efflux. Instead, efflux occurs by either simple diffusion or by a combination of diffusion and another very low-affinity carrier.

*PGE<sub>2</sub> efflux occurs by simple diffusion*

We used TGBz T34 to further isolate the efflux process of PGE<sub>2</sub>. As shown in Figure 4C, we allowed PGE<sub>2</sub> uptake to proceed to different time points (3, 6, 9, 20, and 35 minutes) and then added 25 μM T34 to stop the accumulation. The intracellular concentrations of PGE<sub>2</sub> at different time points were calculated by dividing the total amount of intracellular PGE<sub>2</sub> on the dish by the total volume of cells, based on cell number counts and published individual cell volume (Schneider et al., 2000; Hill et al., 2004). Since the addition of inhibitor involved removing extracellular tracer PGE<sub>2</sub>, the intracellular PGE<sub>2</sub> concentration at the point of inhibitor addition approximates the outwardly-directed PGE<sub>2</sub> gradient. Initial PGE<sub>2</sub> efflux rates at various PGE<sub>2</sub> outward gradients are shown in Figure 4D.

Initial PGE<sub>2</sub> efflux rates from Figure 4C and 4D were linear as a function of the outwardly-directed PGE<sub>2</sub> gradients over the range of 0 to 30 nM, with a "y" intercept not significantly different from zero (efflux rate = [(0.0106)(gradient)] + 0.048, r<sup>2</sup> = 0.98, p < 0.05). This linearity held true even when the intracellular PGE<sub>2</sub> concentration was extended to almost 800 nM, i.e. 10 fold the K<sub>m</sub> of PGT for PGE<sub>2</sub> (data not shown). From the slope of the relationship, we generated a range of permeability coefficients for PGE<sub>2</sub> efflux of 1.2 to 5.3 x 10<sup>-6</sup> cm/sec, based on the range of MDCK cell volumes reported in the literature (Schneider et al., 2000; Hill et al., 2004). Using wild-type MDCK cells that do not express PGT, we obtained a permeability coefficient for PGE<sub>2</sub> influx (by simple diffusion) of 0.45 x 10<sup>-6</sup> cm/sec (data not shown). The ratio of the influx-to-efflux permeability coefficients was thus in the range 2.7 to 11.7.

## Discussion

Organic dyes and nonsteroidal anti-inflammatory drugs have been known to inhibit PGT for some time (Kanai et al., 1995). This is the first report of a new class of PGT inhibitors developed by screening small molecules. The compound library was built by solid-phase combinatorial chemistry and screened by Microbeta scintillation counting on multi-well plates. This strategy allowed us to find a PGT inhibitor, TGBz T34, with a  $K_i$  of  $3.7 \pm 0.2 \mu\text{M}$ , after screening fewer than 2000 compounds. At  $25 \mu\text{M}$ , TGBz T34 exerted full inhibition of  $\text{PGE}_2$  transport by PGT. Double reciprocal analysis revealed that T34 is a competitive inhibitor of PGT. Because T34 eliminated PGT transport activity rapidly, it probably inhibits PGT directly rather than indirectly via metabolic effects.

The  $K_i$  of TGBz T34 is similar to that of bromocresol green (Kanai et al., 1995). TGBz T34 has the potential to be improved because there are three moieties around the scaffold that can be modified. Native substrates of PGT all possess a COOH group and are negatively charged at physiological pH (Schuster, 1998). The carboxylic group at carbon 1 is critical for PG binding to PGT (Eling et al., 1977; Schuster et al., 2000), which is probably why group B (Supplemental Data, Figure 3S) was associated with inhibition.

Some investigators have hypothesized that PGT represents the mechanism by which PGs efflux from cells (Funk, 2001; Banu et al., 2003), whereas others have invoked active pumps such as MRP4 (Reid et al., 2003). Identification of these inhibitors enabled us to investigate the mechanism of  $\text{PGE}_2$  transport in a more refined way. As reported previously by our laboratory (Chan et al., 1998; Schuster, 2002) and in the

present study, a normal time course of PGE<sub>2</sub> transport is divided into three phases (Figure 4). Phase 1 is rapid uptake, phase 2 is overshoot, and phase 3 is equilibrium phase.

Addition of T34 at the point of peak intracellular PGE<sub>2</sub> accumulation demonstrated that PGE<sub>2</sub> efflux is ongoing during PGT-mediated uptake (Figure 4) i.e. the accumulation of intracellular PGE<sub>2</sub> in phase 1, and the maintenance of the equilibrium in phase 3, are due to the active pumping of PGE<sub>2</sub> into the cells by PGT against a background efflux.

Using TGBz T34 we were able to isolate the components of PGE<sub>2</sub> efflux. After loading cells with PGE<sub>2</sub> and blocking PGT-mediated uptake with T34, the PGE<sub>2</sub> efflux rate was linear as a function of the estimated outwardly-directed PG gradient, even at high concentrations. These data indicate that PGE<sub>2</sub> efflux, at least from the compartment loaded by PGT, most likely occurred by simple diffusion.

The hypothesis that PGE<sub>2</sub> efflux occurs by simple diffusion is further supported by our calculated permeability coefficients. At physiological pH, PGs are negatively charged. Because the cell interior is electrically negative, the electrical driving force for simple diffusion is in favor of PGE<sub>2</sub> efflux. The theoretical ratio of the permeability coefficients for diffusional efflux compared to diffusional influx, based on the membrane potential, is in the range of 2 – 11 (Schuster, 2002). The ratios we generated agree with this range. Taken together, our data support a model of PGE<sub>2</sub> transport as a pump (PGT-mediated influx) - leak (diffusional efflux) system.

In summary, we have reported developing a new class of PGT inhibitors by screening a library of small molecules. The most potent of these allowed us to clarify the mechanisms for influx and efflux of PGE<sub>2</sub>. This compound and others should form the basis for further pharmacological investigation of PG transport and should serve as lead

compounds in developing therapeutic agents.

**References:**

Alm A (1998) Prostaglandin derivatives as ocular hypotensive agents. *Progress in Retinal and Eye Research* **17**:291-312.

Banu SK, Arosh JA, Chapdelaine P and Fortier MA (2003) Molecular cloning and spatio-temporal expression of the prostaglandin transporter: a basis for the action of prostaglandins in the bovine reproductive system. *Proc Natl Acad Sci U S A* **100**:11747-11752.

Bao Y, Pucci ML, Chan BS, Lu R, Ito S and Schuster VL (2002) Prostaglandin transporter PGT is expressed in cell types that synthesize and release prostanoids. *American Journal of Physiology* **282**:F1103-1110.

Bito LZ and Salvador EV (1976) Effects of anti-inflammatory agents and some other drugs on prostaglandin biotransport. *J.Pharmacol.Exp.Ther.* **198**:481-488.

Blatteis CM and Sehic E (1997) Fever: How may circulating pyrogens signal the brain? *News in Physiological Sciences.* **12**:1-9.

Bley KR, Hunter JC, Eglen RM and Smith JA (1998) The role of IP prostanoid receptors in inflammatory pain. *Trends Pharmacol Sci* **19**:141-147.

Bork JT, Lee JW, Khersonsky SM, Moon HS and Chang YT (2003a) Novel orthogonal strategy toward solid-phase synthesis of 1,3,5-substituted triazines. *Org Lett* **5**:117-120.

Bork JY, Lee JW and Chang YT (2003b) Palladium-catalyzed cross-coupling reaction of resin-bound chlorotriazines. *Tetrahedron Letters* **44**:6141-6144.

Bos CL, Richel DJ, Ritsema T, Peppelenbosch MP and Versteeg HH (2004) Prostanoids and prostanoid receptors in signal transduction. *Int J Biochem Cell Biol* **36**:1187-1205.

Chan BS, Endo S, Kanai N and Schuster VL (2002) Identification of lactate as a driving force for prostanoid transport by prostaglandin transporter PGT. *Am J Physiol* **282**:F1097-F1102.

Chan BS, Satriano JA, Pucci ML and Schuster VL (1998) Mechanism of prostaglandin E2 transport across the plasma membrane of HeLa cells and *Xenopus* oocytes expressing the prostaglandin transporter "PGT". *J Biol Chem* **273**:6689-6697.

Clyman RI, Mauray F, Roman C and Rudolph AM (1978) PGE2 is a more potent vasodilator of the lamb ductus arteriosus than is either PGI2 or 6 keto PGF1alpha. *Prostaglandins* **16**:259-264.



Coceani F and Olley PM (1988) The control of cardiovascular shunts in the fetal and perinatal period. *Can J Physiol Pharmacol* **66**:1129-1134.

Eling TE, Hawkins HJ and Anderson MW (1977) Structural requirements for, and the effects of chemicals on, the rat pulmonary inactivation of prostaglandins. *Prostaglandins* **14**:51-60.

Endo S, Nomura T, Chan BS, Lu R, Pucci ML, Bao Y and Schuster VL (2002) Expression of PGT in MDCK cell monolayers: polarized apical localization and induction of active PG transport. *American Journal of Physiology* **282**:F618-F622.

Epstein M (1986) *Prostaglandins and the kidney. American journal of medicine; v. 80, no. 1A, 1986.* Technical Publishing, New York, N.Y.

Funk CD (2001) Prostaglandins and leukotrienes: advances in eicosanoid biology. *Science* **294**:1871-1875.

Helliwell RJ, Adams LF and Mitchell MD (2004) Prostaglandin synthases: recent developments and a novel hypothesis. *Prostaglandins Leukotrienes and Essential Fatty Acids* **70**:101-113.

- Hill DA, Chiosea S, Jamaluddin S, Roy K, Fischer AH, Boyd DD, Nickerson JA and Imbalzano AN (2004) Inducible changes in cell size and attachment area due to expression of a mutant SWI/SNF chromatin remodeling enzyme. *J Cell Sci* **117**:5847-5854.
- Jacquemin E, Hagenbuch B, Stieger B, Wolkoff AW and Meier PJ (1994) Expression cloning of a rat liver Na<sup>+</sup>-independent organic anion transporter. *Proc Natl Acad Sci U S A* **91**:133-137.
- Kanai N, Lu R, Satriano JA, Bao Y, Wolkoff AW and Schuster VL (1995) Identification and characterization of a prostaglandin transporter. *Science* **268**:866-869.
- Khersonsky SM, Jung DW, Kang TW, Walsh DP, Moon HS, Jo H, Jacobson EM, Shetty V, Neubert TA and Chang YT (2003) Facilitated forward chemical genetics using a tagged triazine library and zebrafish embryo screening. *J Am Chem Soc* **125**:11804-11805.
- Moon HS, Jacobson EM, Khersonsky SM, Luzung MR, Walsh DP, Xiong W, Lee JW, Parikh PB, Lam JC, Kang TW, Rosania GR, Schier AF and Chang YT (2002) A novel microtubule destabilizing entity from orthogonal synthesis of triazine library and zebrafish embryo screening. *J Am Chem Soc* **124**:11608-11609.

- Narumiya S, Sugimoto Y and Ushikubi F (1999) Prostanoid receptors: structures, properties, and functions. *Physiological Reviews* **79**:1193-1226.
- Nomura T, Lu R, Pucci ML and Schuster VL (2004) The two-step model of prostaglandin signal termination: in vitro reconstitution with the prostaglandin transporter and prostaglandin 15 dehydrogenase. *Mol Pharmacol* **65**:973-978.
- Reid G, Wielinga P, Zelcer N, van der Heijden I, Kuil A, de Haas M, Wijnholds J and Borst P (2003) The human multidrug resistance protein MRP4 functions as a prostaglandin efflux transporter and is inhibited by nonsteroidal antiinflammatory drugs. *Proc Natl Acad Sci U S A* **100**:9244-9249.
- Samad TA, Sapirstein A and Woolf CJ (2002) Prostanoids and pain: unraveling mechanisms and revealing therapeutic targets. *Trends Mol Med* **8**:390-396.
- Schneider SW, Pagel P, Rotsch C, Danker T, Oberleithner H, Radmacher M and Schwab A (2000) Volume dynamics in migrating epithelial cells measured with atomic force microscopy. *Pflugers Arch* **439**:297-303.
- Schuster VL (1998) Molecular mechanisms of prostaglandin transport. *Ann Review of Physiology* **60**:221-242.

Schuster VL (2002) Prostaglandin Transport. *Prostaglandins and Other Lipid Mediators* **68-69**:633-647.

Schuster VL, Itoh S, Andrews SW, Burk RM, Chen J, Kedzie KM, Gil DW and Woodward DF (2000) Synthetic modification of prostaglandin f(2alpha) indicates different structural determinants for binding to the prostaglandin f receptor versus the prostaglandin transporter. *Molecular Pharmacology* **58**:1511-1516.

Smith GCS, Coleman RA and McGrath JC (1994) Characterization of dilator prostanoid receptors in the fetal rabbit ductus arteriosus. *Journal of Pharmacology & Experimental Therapeutics* **271**:390-396.

Stjernerchantz J (1995) Prostaglandins as ocular hypotensive agents; development of an analogue for glaucoma treatment. *Advances in Prostaglandin Thromboxane and Leukotriene Research* **23**:63-68.

Stjernerchantz J (2004) Studies on ocular inflammation and development of a prostaglandin analogue for glaucoma treatment. *Experimental Eye Research* **78**:759-766.

Susanna R, Jr., Chew P and Kitazawa Y (2002) Current status of prostaglandin therapy: latanoprost and unoprostone. *Survey in Ophthalmology* **47 Suppl 1**:S97-104.

Sweet DH, Wolff NA and Pritchard JB (1997) Expression cloning and characterization of ROAT1. The basolateral organic anion transporter in rat kidney. *J.Biol.Chem.* **272**:30088-30095.

Ulmann A, Silvestre L, Chemama L, Rezvani Y, Renault M, AguilleauCJ. and Baulieu EE (1992) Medical termination of early pregnancy with mifepristone (RU 486) followed by a prostaglandin analogue. Study in 16,369 women. *Acta Obstet.Gynec.Scand.* **71**:278-283.

Uttamchandani M, Walsh DP, Khersonsky SM, Huang X, Yao SQ and Chang YT (2004) Microarrays of tagged combinatorial triazine libraries in the discovery of small-molecule ligands of human IgG. *J Comb Chem* **6**:862-868.

Vanegas H and Schaible HG (2001) Prostaglandins and cyclooxygenases [correction of cyclooxygenases] in the spinal cord. *Prog Neurobiol* **64**:327-363.

Wang JL, Cheng HF, Zhang MZ, McKanna JA and Harris RC (1998) Selective increase of cyclooxygenase-2 expression in a model of renal ablation. *Am.J.Physiol.* **275**:F613-F622.

Yokoyama C, Yabuki T, Shimonishi M, Wada M, Hatae T, Ohkawara S, Takeda J, Kinoshita T, Okabe M and Tanabe T (2002) Prostacyclin-deficient mice develop

ischemic renal disorders, including nephrosclerosis and renal infarction.

*Circulation* **106**:2397-2403.

### Footnotes

Grant support: Supported by NIH grants R01DK049688 and P50DK064236 to V. L. Schuster.

## Legends for Figures

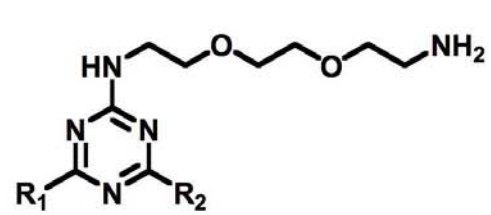
1. Structures of the main scaffolds.
2. Structures of the three most potent TGBz compounds and their degree of PGT inhibition.
3. Inhibitory effect of TGBz T34 on PGT-mediated PGE<sub>2</sub> uptake. The TGBz T34 inhibition constant and its mode of inhibition were determined by varying PGE<sub>2</sub> concentration at fixed levels of TGBz T34 equal to 0 μM (*circle*), 3 μM (*square*), and 6 μM (*diamond*). Double-reciprocal plots for TGBz T34 inhibition demonstrate that TGBz T34 is a competitive inhibitor of PGT with a  $K_i$  value of  $3.7 \pm 0.2$  μM.
  - 4A. Time course of PGE<sub>2</sub> uptake by MDCK cells stably expressing PGT in the presence of TGBz T34 at various concentrations. TGBz T34 was added at the beginning of each time course at 0 μM (*square*), 1 μM (*circle*), 4 μM (*diamond*), 10 μM (*up triangle*), 25 μM (*down triangle*).
  - 4B. Time course of PGE<sub>2</sub> uptake by PGT in MDCK cells stably expressing PGT without TGBz T34 (*open circle*) and with 25 μM TGBz T34 added at the time point at which intracellular PGE<sub>2</sub> reached its peak level (*solid circle*).
  - 4C. Time course of PGE<sub>2</sub> uptake by PGT in MDCK cells stably expressing PGT with 25 μM TGBz T34 added at different time points on the uptake time course: 3 minutes (*up triangle*), 6 minutes (*down triangle*), 9 minutes (*diamond*), 20 minutes (*circle*), and 35 minutes (*square*).



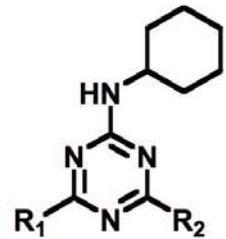
4D. Initial PGE<sub>2</sub> efflux velocities ( $V_i$ ) and their corresponding intracellular PGE<sub>2</sub> concentrations as obtained from the data of panel C.

Table 1.  $K_i$  Values of TGBz Inhibitors of PGT

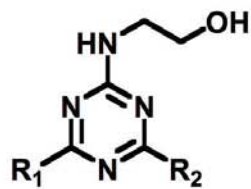
Compounds	$K_i$ ( $\mu\text{M}$ )
T34	$3.7 \pm 0.2$
T41	$6.2 \pm 0.7$
T07	$12.5 \pm 1.5$



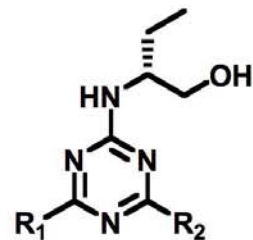
**AA**



**BN**



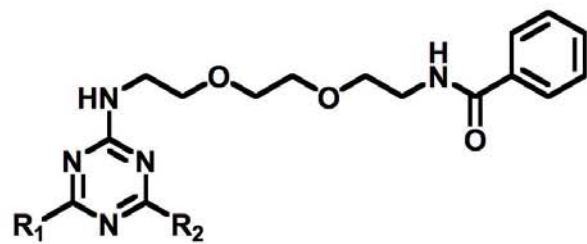
**EA**



**RT**



**TF**



**TGBz**

Figure 1



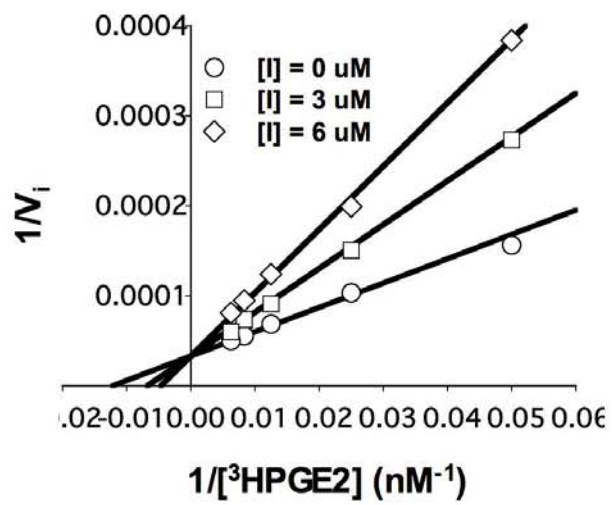
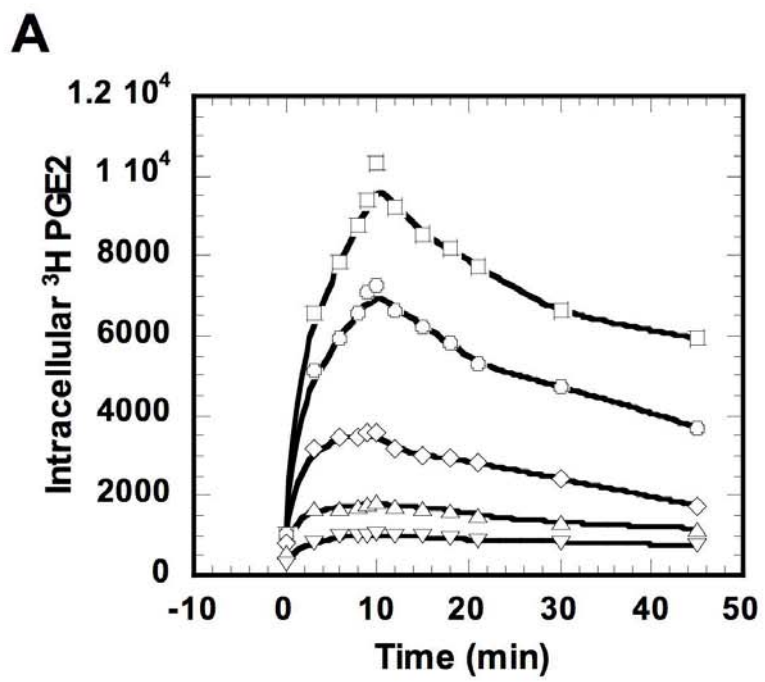
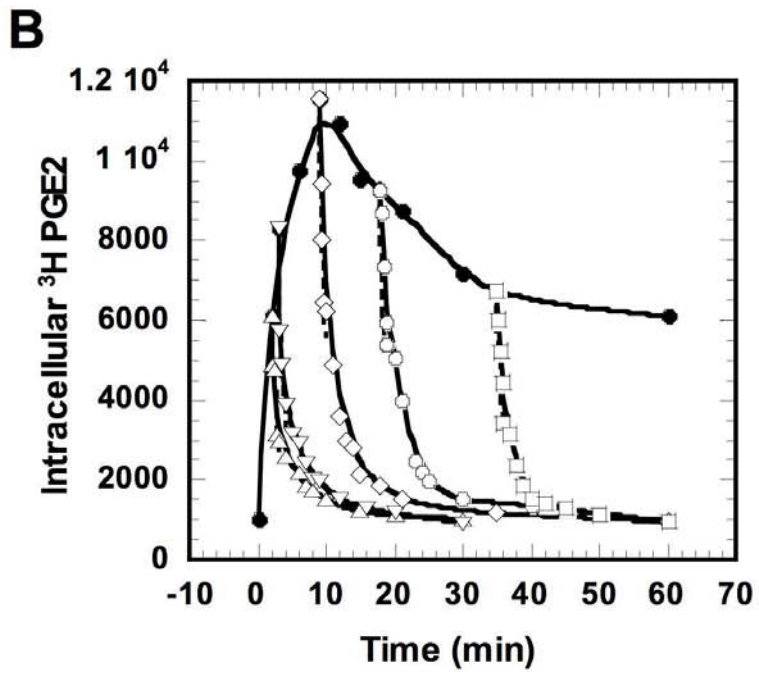


Figure 3



**Figure 4A**



**Figure 4B**

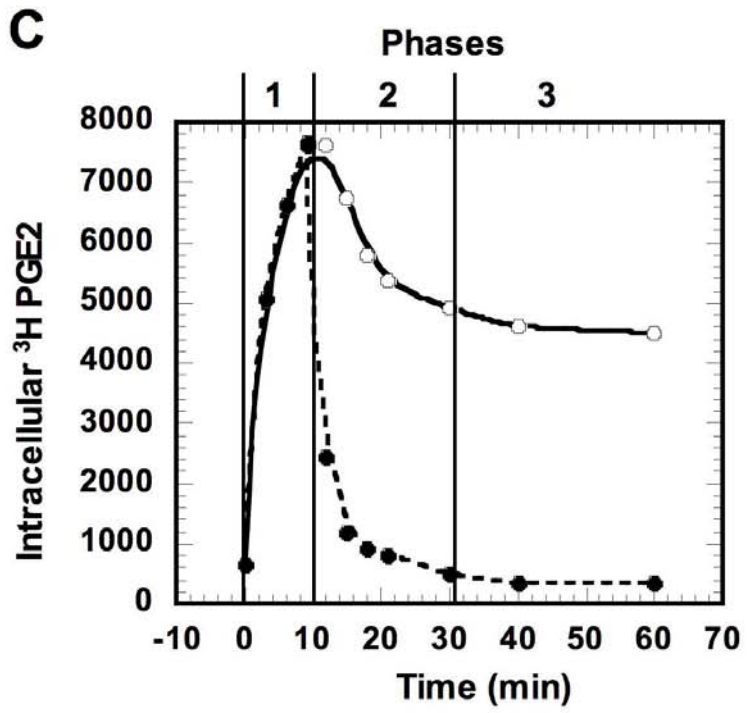


**Figure 4C**



**D**

<b>Time (min)</b>	<b><math>\Delta</math>[PGE2] (nM)</b>	<b><math>V_i</math> (fmoles/s)</b>
<b>3</b>	<b>12.884</b>	<b>0.19217</b>
<b>6</b>	<b>17.754</b>	<b>0.24083</b>
<b>9</b>	<b>25.120</b>	<b>0.32091</b>
<b>20</b>	<b>19.915</b>	<b>0.24794</b>
<b>35</b>	<b>14.189</b>	<b>0.19359</b>

**Figure 4D**